



Nanoghosts: Mesenchymal Stem cells derived nanoparticles as a unique approach for cartilage regeneration

D. D'Atri ^a, L. Zerrillo ^b, J. Garcia ^c, J. Oieni ^a, Y. Lupu-Haber ^a, T. Schomann ^b, A. Chan ^b, L. J. Cruz ^b, L.B. Creemers ^c, Marcelle Machluf ^{a,*}

^a Faculty of Biotechnology and Food Engineering, Technion Israel Institute of Technology, Technion City, Haifa, Israel

^b Department of Radiology, Leiden University Medical Center (LUMC), Albinusdreef 2, 2333, ZA, Leiden, the Netherlands

^c Department of Orthopaedics, University Medical Center, 3584, CX, Utrecht, the Netherlands



ABSTRACT

Osteoarthritis (OA) is a chronic degenerative disease, which affects the joints and is characterized by inflammation, cartilage loss and bone changes. Nowadays, there are no treatments for OA, and current therapies are focused on relieving the symptoms. As a new therapy approach, micro and nanoparticles have been extensively explored and among all the studied particles, the use of cell-membrane-based particles is expanding. Another promising approach studied to treat OA, is the use of mesenchymal stem cells (MSCs) which play an important role modulating inflammation. We developed a novel kind of MSCs' cytoplasmic-membrane-based nanoparticles, termed nano-ghosts (NGs).

Retaining MSCs' surface properties and lacking cells' internal machinery allow the NGs to have immunomodulatory capacity and to be immune-evasive while not susceptible to host-induced changes.

In this study, we demonstrate NGs' ability to target cartilage tissues, *in vitro* and *in vivo*, while modulating the inflammatory process. *In vivo* studies demonstrated NGs ability to act as an immunomodulatory drug slowing down cartilage degeneration process.

Our proof-of-concept experiments show that NGs system is a versatile nano-carrier system, capable of therapeutics loading, with targeting capabilities towards healthy and inflamed cartilage cells. Our results, along with previously published data, clearly reveal the NGs system as a promising nano-carrier platform and as a potential immunomodulatory drug for several inflammation-related diseases.

1. Introduction

Osteoarthritis (OA) involves processes such as cartilage degradation, subchondral bone sclerosis, and osteophyte formation [1,2]. Although the causes that lead to the onset of OA are unknown [3], it is manifested with degenerative and inflammatory processes, which promote the progression of the disease [3–6]. The extracellular matrix (ECM), which is the main component of the cartilage tissue, is typically maintained under steady and low turnover conditions until OA onsets. The activation of the cells, due to inflammatory pathways, may induce overproliferation that leads to a phenotypic shift, apoptosis, and aberrant expression of inflammation-related cytokine and enzymes. However, OA's origin and its mechanism of progression are still unknown. Therefore, there are currently no efficient treatments to inhibit cartilage degradation or arresting the disease progression. Current treatments, including physical activity, weight managing, anti-inflammatory therapeutics (e.g., NSAIDs or corticosteroids) are mainly focused on relieving

the symptoms such as pain, and in severe cases joint replacement is performed [1,7]. New emerging therapies include the use of strontium ranelate (that inhibits subchondral bone resorption by regulating the activity of the metalloproteinases), AAV-mediated delivery of IL1RA, and regenerative therapies. Among the cell-based therapies, the mesenchymal stem cells (MSCs) are the cells most frequently used as they have shown to have regenerative effects, although their major role nowadays is considered to be immune-suppressive.

MSCs are known to be involved in processes of wound healing, immunomodulation, and homing capabilities in multiple inflammation sites. For these reasons, they have been tested in clinical trials. MSCs' homing and immune-modulatory capabilities are largely associated with membrane composition and membrane orientation.

Nonetheless, cell-based therapy is generally associated with several drawbacks. The number of cells needed for the injection is still under study, and it has been showed that a dose of 10^7 cells can lead to scarring and formation of extra bone tissue [8]. In addition, the number of

* Corresponding author at: The Laboratory of Cancer Drug Delivery & Mammalian Cell Technology, Faculty of Biotechnology & Food Engineering, Technion-Israel Institute of Technology, Haifa 32000, Israel.

E-mail address: machlufm@tx.technion.ac.il (M. Machluf).

required injections is under investigation because the function and the potency of the MSCs are variable as well as their source.

In previous research, we reported the potential of a new biomimetic tumor-targeted platform, called nanoghosts (NGs), which can work as vehicles for drug-delivery. NGs are MSC-membrane-based nanovesicles. The production of NGs involves different steps starting from the removal of the MSCs' cytoplasm, which leads to formation of inanimate ghosts cells, which are hence downscaled until a nano-scale dimension is reached.

The immunomodulatory capacity of MSCs is retained by the NGs and, particularly, the ability to home to inflammatory tissues.

However, as the NGs lack the internal cell machinery, unlike the cells of origin, they do not respond to external stimuli nor are they susceptible to host-induced changes [9–12]. In this study, we aim to demonstrate the safety and the efficacy of using NGs as an immunomodulatory drug for the treatment of OA. To this end, chondrocytes-like cells lines and primary cells were first investigated *in vitro* and, finally we studied the effect of intra-articular injection of NGs in OA mice. We provide evidence on the efficacy of the NGs in reducing inflammation acting as modulatory of the related processes *in vitro* and preventing bone formation and cartilage degradation *in vivo*.

2. Material and methods

2.1. Cells cultures

Unless stated otherwise, all cell culture media, growth factors and antibiotics were purchased from Biological Industries (Bet-Ha'Emek, Israel).

MSCs were purchased from Lonza (Basel, Switzerland) and cultured in alpha-MEM, supplemented with 10% fetal bovine serum (FBS), 0.8% amphotericin-B, 1% penicillin-streptomycin (P/S) and 5 ng/mL of basic fibroblast growth factor (bFGF, Peprotech, Rehovot, Israel). The cells were seeded at 2500 cells/cm², the medium was changed every two days and the cells were harvested at 70% confluence. C-28/I2 cells (kindly provided by Dr. Mary B. Goldring at the Hospital for Special Surgery, New York, NY, and can be purchased from Millipore (cat # SCC042) and Prof. L.B. Creemers Department of Orthopedics, University Medical Center Utrecht, Utrecht, the Netherlands) and were cultured in DMEM: F12 supplemented with 10% FBS, 0.8% amphotericin-B, 1% P/S and 2 mM of Glutamine. Cells were seeded at the density of 10³ cells/cm², the medium was changed every two days and harvested every 2–3 days. Osteoarthritic human chondrocytes (hACs: kindly provided by Prof. L.B. Creemers Department of Orthopedics, University Medical Center Utrecht, Utrecht, the Netherlands) were cultured in DMEM:F12 supplemented with 10% FBS, 1% P/S and 1% Ascorbic Acid 2-phosphate (Sigma, A8960) and 1% Glutamine. Human smooth muscle cells (hSMCs, #PCS-420-012, ATCC) were cultured in DMEM high glucose (Sigma Aldrich) supplemented with 10% FBS, 1% P/S solution and 0.8% amphotericin-B solution. All cells were harvested using PBS-EDTA and 0.05% Trypsin. Cells were cultured at 37 °C in a humidified incubator with 5% CO₂.

2.2. Nanoghost production and characterization

The NGs were produced as previously published [10–12]. Briefly, NGs were prepared from the cytoplasmic membrane of MSCs in a multi-step process, which involve hypotonic treatment, homogenization, sonication, filtration and PEGylation [10–12]. For *in vitro* and *in vivo* tracking, fluorescent NGs were obtained by incubating the MSCs with the fluorescent lipophilic tracers DiO, DiD or DiR (Life Technologies™) for three hours and after incubation period the labeled NGs were prepared as previously published [10–13]. The following physical qualities of the NGs were characterized: size and size distribution using the NanoSight 3000 (Malvern Instruments, Malvern-Worcestershire, UK); surface charge of the NGs, in particular the Z-potential was characterized using

Zetasizer Nano-Series (Malvern Instrument). NGs morphology and size were also characterized using FEI T12 G2 Cryo-Transmission Electron Microscopy (Cryo-TEM) operated at 120 kV and using Atomic Force Microscope (AFM) JPK Nano Wizard 3 in AC Mode using OMCL-AC160TS silicon probes (Olympus, City, Country) with a resonance of 300 kHz and constant spring of 30 N/m. Cryo-TEM Images were recorded on a Gatan US1000 2 k × 2 k high-resolution cooled CCD camera using Digital Micrograph software, while AFM images were analyzed using Gwyddion SPM Software (Supported by Department of Nanometrology, Czech Metrology Institute (Brno, CZ)).

NGs concentration was measured by phospholipids quantification using the LabAssay phospholipid Kit (Wako Osaka Japan) according to the manufacturer protocol and in the whole study the concentration of NGs is presented as phospholipid (*w/v*).

2.3. NG interaction with cells

NGs targeting ability was tested with a wide variety of cells using several controls (see *Supplementary Data*). Our attention was particularly focused towards chondrocytes and chondrocytes-like cells. C-28/I2, hACs and hSMCs were plated at the density of 10⁴ cells/cm² in a 24 well plate and cultured overnight. Subsequently, the medium was replaced with a serum free medium supplemented with 5 µg/mL of fluorescence labeled NGs (DiD, DiO or DiR) and incubated at 37 °C for 15 min. To label the nuclei, the cells were incubated with DAPI (300 nM) at RT for 20 min. To determine the cellular uptake of the NGs, cells were washed four times with PBS and harvested with 0.05% of Trypsin. The median fluorescent intensity (MFI) was measured using a flow cytometer (BD FACSCalibur™, Biologcal Industries, San Diego, CA). Cells that were not incubated with fluorescence labeled NGs were used as a background control, while the hSMCs where used as a non-mesenchymal control for the targeting. The median fluorescent intensity of targeted cells was measured and analyzed using FlowJo 10 software.

For further confirmation of the NGs targeting properties, and their cellular uptake the experiments were repeated using the same parameters described above but the fluorescence was measured by imaging flow cytometry (AMNIS IMAGESTREAM®X MARK II, Luminex Corporation) and the results were analyzed using the software IDEAS.

2.4. Imaging of NGs' binding

C-28/I2 and hAC were seeded at a density of 50³ cells/cm² in 4 chamber glass bottom dishes (Cellvis) and cultured overnight. The following morning the medium was replaced with a serum-free medium containing 5 µg lipid/mL of DiD (or DiO) labeled NGs. Cells were incubated with NG-enriched medium for 30 min. Cells were then washed three times with PBS and fixed on ice with 4% PFA for 20 min. Cells were washed again for three times with PBS and permeabilized with 0.1% solution of Triton-X for 5 min and washed again. The permeabilized cells were then incubated with phalloidin-TRITC (5 µM) at RT for one hour. Subsequently, cells were washed three times with PBS and the nuclei were stained with Hoechst 33342 (2.5 µg/mL Thermo-Fischer) for 20 min followed by with three washes with PBS. Cells were imaged using LEICA SP8 confocal scanning laser microscope for hAC and LSM710-Inverted confocal for C-28/I2.

2.5. Nitric oxide quantification

The levels of the secreted nitric oxide (NO) were measured using the Griess assay (Promega G2930) [14,15]. hACs and C-28/I2 cells were seeded at a density of 20³ cells/cm² in a 96 well and incubated overnight. One day after seeding, the medium was replaced with fresh medium supplemented with 10 ng/mL of TNFα (Prepotech) and cultured up to three days. Untreated cells served as a negative control. After three days the medium of each sample was collected and the concentration of NO was analyzed using a Griess Reagent System (Promega, G2930)

according to the manufacturer's protocol. The absorbance was measured at 535 nm using a Synergy H1 Hybrid Multi-Mode Reader (BioTek, Winooski, Vermont, USA).

2.6. Cell viability

hACs and C-28/I2 were seeded at a density of 20^3 cells/cm² in a 96 well plate and incubated overnight. The medium was supplemented with 5 µg/mL of NGs or ethanol as a positive control for the apoptosis [16] or 0.1% solution of Triton-X as a positive control for the necrosis 24 h later [17,18]. Cell death was measured using the Apotox-Glo triplex Assay (Promega, #G6320) and the results were analyzed according to the manufacturer's protocol. The absorbance and the luminescence were measured using a Synergy H1 Hybrid Multi-Mode Reader (BioTek, Winooski, Vermont, USA).

2.7. Quantification of PGE2 and pro-inflammatory cytokines

Cells were cultured as described above and the medium was changed three days after TNFα stimulation (10 ng/mL), and NGs (5 µg lipid/mL) were added to the wells for 24 h. Next, the medium of untreated cells and stimulated cells was collected and analyzed for presence of pro-inflammatory factors by ELISA. PGE2 (Prostaglandin E2 ELISA Kit – Monoclonal, Cayman, #514010), IL6 (Human IL-6 DuoSet ELISA, R&D, DY206) and IL8 (Human IL-8/CXCL8 DuoSet ELISA, R&D, DY208). Cytokine and PGE2 concentrations were measured using an ELISA assay, and absorbance was measured using a Synergy H1 Hybrid Multi-Mode Reader (BioTek, Winooski, Vermont, USA). All the results were analyzed according to the manufacturer's protocol.

2.8. mRNA isolation and qRT-PCR

Cells were seeded at a density of 20^3 cells/cm² in a 24 well plate and incubated overnight. After 24 h, the medium was changed to medium supplemented with 5 µg/mL of NGs for 24 h. RNA was isolated and purified using TRI-Reagent (Sigma Aldrich #T9424) according to the manufacturer's protocol. RNA concentration and quality were determined using a NanoDrop ND1000. cDNA was synthesized from total RNA in a 20 µL reaction volume using TaqMan MicroRNA Reverse transcription kit (ThermoFischer). qPCR was performed in 20 µL reactions using a DyNAamo ColorFlash SYBR Green qPCR Kit (ThermoFisher, #F416S) according to the manufacturer's guidelines. 18S housekeeping gene was amplified and other genes data were normalized on 18SrRNA levels. Relative gene expression was calculated according to the $2^{-\Delta CT}$ formula.

2.9. In vivo intra-articular injection of NGs in OA

All animal studies were conducted in collaboration with Percuros B. V. Leiden within the group of Dr. A. Chan. Animal care and handling were in accordance with the guidelines and regulations as stipulated by the Dutch Experiments on Animals Act (WoD) and the European Directive on the Protection of Animals Used for Scientific Purposes (2010/63/EU). All applicable institutional and national guidelines for the care and use of animals were followed. Mice were housed in the Animal Care Facility of Leiden University Medical Center (LUMC, the Netherlands) under standard housing conditions (group cages with enriched environment, food and water *ad libitum*; diurnal light cycle [12 h light, 12 h dark], temperature 21 °C; humidity 60%). The use of the animals was approved by the Animal Experiments Committee of the Leiden University Medical Center (permit numbers AVD1160020171405 and AVD1160020171405_18.042-01).

For the *in vivo* experiments, a total of 12 male C57BL/6Jico (12 weeks old) were purchased from Charles River, France. Of these, three mice, were kept as healthy untreated control. Six mice underwent a surgical destabilization of the knee medial meniscus (DMM) to induce

OA. Fourteen days post-surgery, three healthy mice, and three operated mice were injected with 8 µL DiR-labeled NGs (1250 µg/mL). While the rest of the mice was injected with the same volume of saline solution (NaCl, 154 mM) as a control for the NG group. All mice were sacrificed 14 days after the NG injection, and the lower limbs were analyzed by µCT-scan. Images were acquired using 10 mm (90 kV/160 mA, 4.5 min) with a resolution of 20 µm. Using the Analyze Direct™ software, (Overland Park, KS-USA) scans were converted in 3D images. Global thresholding was applied to all scans and determined by visual inspection.

2.10. Quantification and histological analysis of NGs retention time in the joint

The *in vivo* imaging system PEARL (Li-Cor, Nebraska, USA) was used to measure the retention time of the NGs inside the joint. The joints were imaged at 0, 2, 4, 6, 8, 12, 24, 48, 72, 168, 240, and 336 h post injection. Fluorescence was measured at 700 nm. After sacrificing the mice, the limbs were fixed for in 4% buffered PFA solution 24 h and subsequently decalcified in 8% formic acid solution for three days and then embedded in paraffin for histological analysis. The knees were then sliced into 5 µm sections and stained with Safranin O/Fast Green examined by optical microscopy to evaluate cartilage damage in the femur and tibia. Joint degeneration was assessed using the OARSI score by two independent scorers, blinded to the conditions. The score goes from 0 (normal joint) to 6 (damaged and calcified cartilage for more than the 75% of the surface). The severity is expressed as summed and/or maximal scores which can be combined for the entire joint or split out between joint compartments.

2.11. Statistical analysis

The statistical analysis was performed using Excel plus Real statistics Analysis tool and GraphPad Prism 7.0. ANOVA (non-parametric) was used to assess the differences between the samples *in vitro*. A Mann-Whitney U test was used to assess the differences between the samples *in vivo*. For all the experiment, $P<0.05$ was considered statistically significant.

3. Results

3.1. Physical characterization of the NGs

A wide NGs characterization was performed to understand chemical and physical characteristic of the nanoparticles. NGs' membrane composition and orientation was widely studied to confirm that NGs did not lose MSCs membrane characteristics and markers (*see Supplementary data*). Furthermore, a deep physical characterization of the particles was performed. NanoSight analysis showed that the NGs exhibited an average diameter of ~200 nm. CryoTEM imaging and AFM analyses revealed that NGs have a spherical shape with a rough surface and confirmed the size of the NGs. Dynamic Light Scattering (DLS) also showed that the average diameter of the particles is ~200 nm while the Z-potential of the particles is -12 mV (Fig. 1 A, B, C).

3.2. Human Articular Chondrocytes and C-28/I2 targeting and co-localization

Fluorescence-labeled NGs were incubated with hACs and C-28/I2 for 15 min, and their uptake was analyzed by flow cytometry and ImageStream. hSMCs were used as control. MSCs NG attachment to hACs (two-fold) and C-28/I2 (three-fold) was three times more efficient compared to the control ($P<0.05$). In addition, when the cells were stimulated with TNFα, the targeting of hACs and C-28/I2 increased by two folds ($P<0.01$) compared to the unstimulated cells (Fig. 2C). ImageStream analysis showed that the NGs could be internalized by the cells. hACs

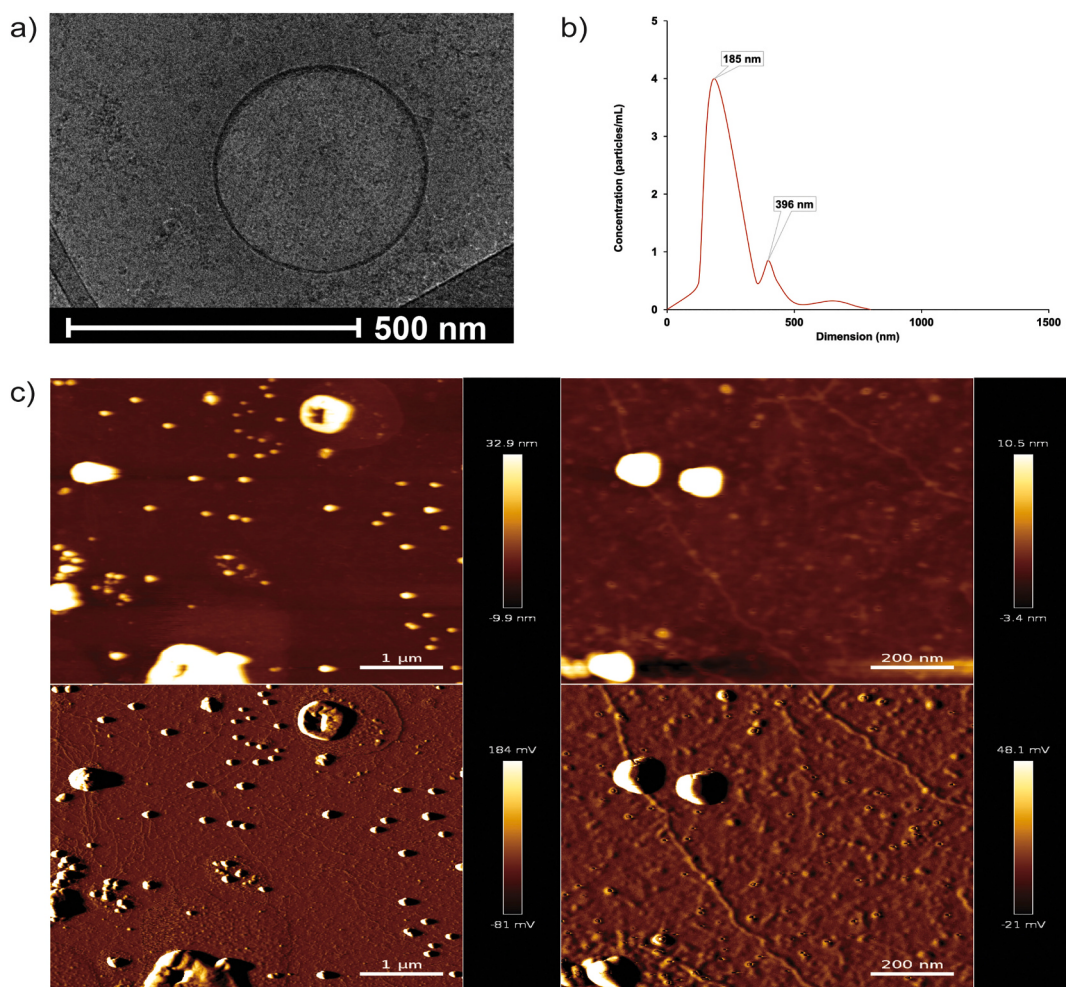


Fig. 1. NGs characterization: a) CryoTEM b) NanoSight Analysis c) AFM Analysis.

internalized twice as many NGs when stimulated with TNF α , and inflamed C-28/I2 showed a three-fold higher internalization than non-stimulated ones. The ImageStream results were confirmed by the confocal imaging where it was shown that NGs accumulate in the cytoplasm of both control and TNF α -stimulated cells (Fig. 2A, B). Live cell imaging using (InCell microscopy) was used to distinguish NGs that were bound to the cell membrane from internalized NGs. To quantify the NGs' uptake, a semi-automatic particle localization routine, which quantifies the fluorescent NGs inside the cells and measures the distance between them and the organelles (Lysosomes and Endosome), was applied. InCell analysis revealed that 53% of NGs were internalized in hACs through the lysosomal pathway after 12 h, while 34% were taken up via the endosomal pathway (13% early and 21% late). NGs that were internalized in C-28/I2 showed similar behavior with 42% colocalization in the lysosome and 18% and 26% in early and late endosome respectively (Fig. 2D).

3.3. In vitro susceptibility to NGs

To determine the biocompatibility of NG, an Alamar blue assay was performed. The result demonstrates that the NGs do not have any effect on the viability of control or TNF α -stimulated cells viability when compared to the positive control (0.1% Triton-X, Fig. 3 A1 and A2).

Moreover, NGs treatment did not lead to apoptosis or necrosis as measured by the Apoptox-Glo Triplex Assay Kit, while in the positive control (treated with 0.1% Triton-X or Ethanol), the apoptosis increased by 60% and necrosis increased by 80% (Fig. 3B and C).

3.4. Effect of NGs on TNF α -induced NO, PGE2 and pro-inflammatory cytokines production

To study the effect of the NGs on the inflammatory process, a Griess assay, an ELISA and RNA expression level analyses were performed. As seen in Fig. 4, the level of NO produced by inflamed cells was significantly reduced by the NGs. For both hACs and C-28/I2, NGs reduced the NO level of treated inflamed cells almost to the levels of the naïve cells. Co-culturing of NGs with unstimulated cells did not show any effect compared to the untreated control (Fig. 4A). To further understand the effect of the NGs on the inflammation process, the levels of pro-inflammatory cytokines and PGE2 were analyzed. As seen from Fig. 4 (B1 and B2), the levels of PGE2s, IL6 and IL8 increased in TNF- α stimulated cells ($P < 0.05$). However, when cells were TNF α stimulated and co-cultured with the NGs, the levels of these cytokines and PGE2 were reduced by three folds for PGE2, 1.6 folds for IL6 and 1.8 folds for IL8 when compared to the untreated inflamed cells. Moreover, as seen in Fig. 4 (C1 and C2), the mRNA expression of PGE2s ($P < 0.001$), COX2 ($P < 0.05$), ADAMTS5 ($P < 0.01$), and MMP13 ($P < 0.001$) significantly decreased in both stimulated hACs and C-28/I2 co-cultured with the NGs, while ACAN expression significantly increased (P value < 0.05). NGs did not have any significant effect on control cells except for the expression of MMP13, which doubled, and the level of ADAMTS5 which decreased by 50% (P value < 0.01).

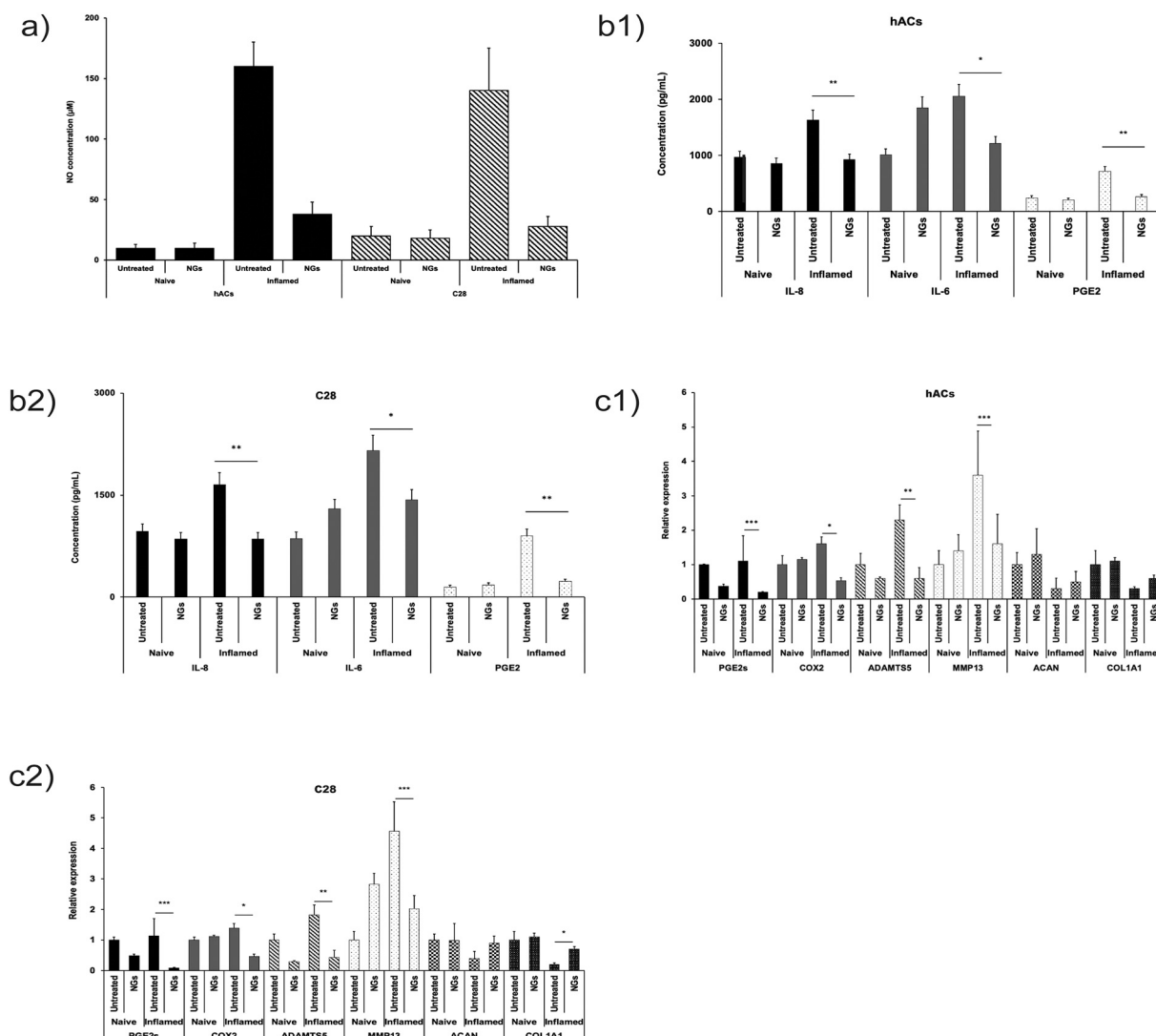


Fig. 2. *In vitro* and *ex vivo* NGs targeting studies.

a) Confocal imaging of human articular chondrocytes target by NGs. From left to right: Untreated cells, naïve cells and inflamed cells. Cells were incubated with 5 μg/mL of NGs, and then stained for different compartments and imaged: Cytoskeleton: cyan, Phalloidin-TRITC; Nuclei: blue, Hoechst 33342; Lysosomes: Green, LAMP1 antibody; NGs: Red, DiR. b) ImageStream flow cytometry of NGs targeting naïve and inflamed human articular chondrocytes and C28. Cells were incubated for 15 min with 5 μg/mL of labeled NGs. NGs targeting hACs: Yellow, DiO; NGs targeting C28: Red, DiR; Cells were unstained. c) Flow cytometry analysis of NGs targeting naïve and inflamed hSMCs, hACs and C28. Cells were incubated for 15 min with 5 μg/mL of labeled NGs (DiO or DiR labeling), then harvested and analyzed d) Colocalization analysis performed using Live Cell Imaging. A semi-automatic particle localization routine to quantify the NGs inside the cells and measures their distance between organelles was applied. e) *Ex-vivo* targeting of human cartilage explant. From left to right: untreated, naïve, inflamed explants. The explants were incubated with 5 μg/mL of DiR labeled NGs than embedded in TCO, cut and imaged. Inflamed explants were incubated with 10 ng/mL of TNFα for 15 days. The images were processed using ImageJ software. f) IVIS analysis of NGs targeting towards rat joints. DiR-NGs (5 μg/mL and 35 μg/mL) were injected into the rat joints and followed with an IVIS for 24 h.

3.5. Ex vivo binding of NGs to cartilage tissue

To assess the NGs binding to cartilage tissue, two different studies were conducted. In the first study, two different concentration of DiR-labeled NGs (5 μg lipid/mL and 35 μg lipid /mL) were injected into the rat joints and followed with an IVIS for 24 h. As seen from Fig. 2F, NGs were able to bind the cartilage and did not leak to the surrounding tissues.

In the second study, NGs were incubated with human osteoarthritic cartilage explants. As seen in Fig. 2 (E1, E2 and E3) and according to the quantification performed via ImageJ the amount of NGs interacting with stimulated tissue was four-fold higher when compared to the unstimulated ones, confirming the *in vitro* targeting results.

3.6. Distribution and preliminary effectivity of NGs in an OA mouse model

To assess the safety and the anti-inflammatory effect of the NGs, *in vivo* studies were performed in a mouse model of instability-induced OA.

DiR-Labeled NG were injected into mice exhibiting OA (Group1), and to healthy mice (Group 2). As a control, mice were injected with saline solution (Group3 and 4). The mice were sacrificed 14 days after injection with DiR-labeled NGs, legs were harvested and scanned using a μCT scanner and stained for Safranin-O/Fast Green and Hematoxylin/Eosin. During the 14 days post injection, mice were followed with NIR imaging. As seen in Fig. 5C, a gradual decline of fluorescence level of the original signal was observed in both healthy and OA joints. The signal loss amounted to up to 40% over time. Furthermore, the NGs remained contained inside the joint as no leakage was observed.

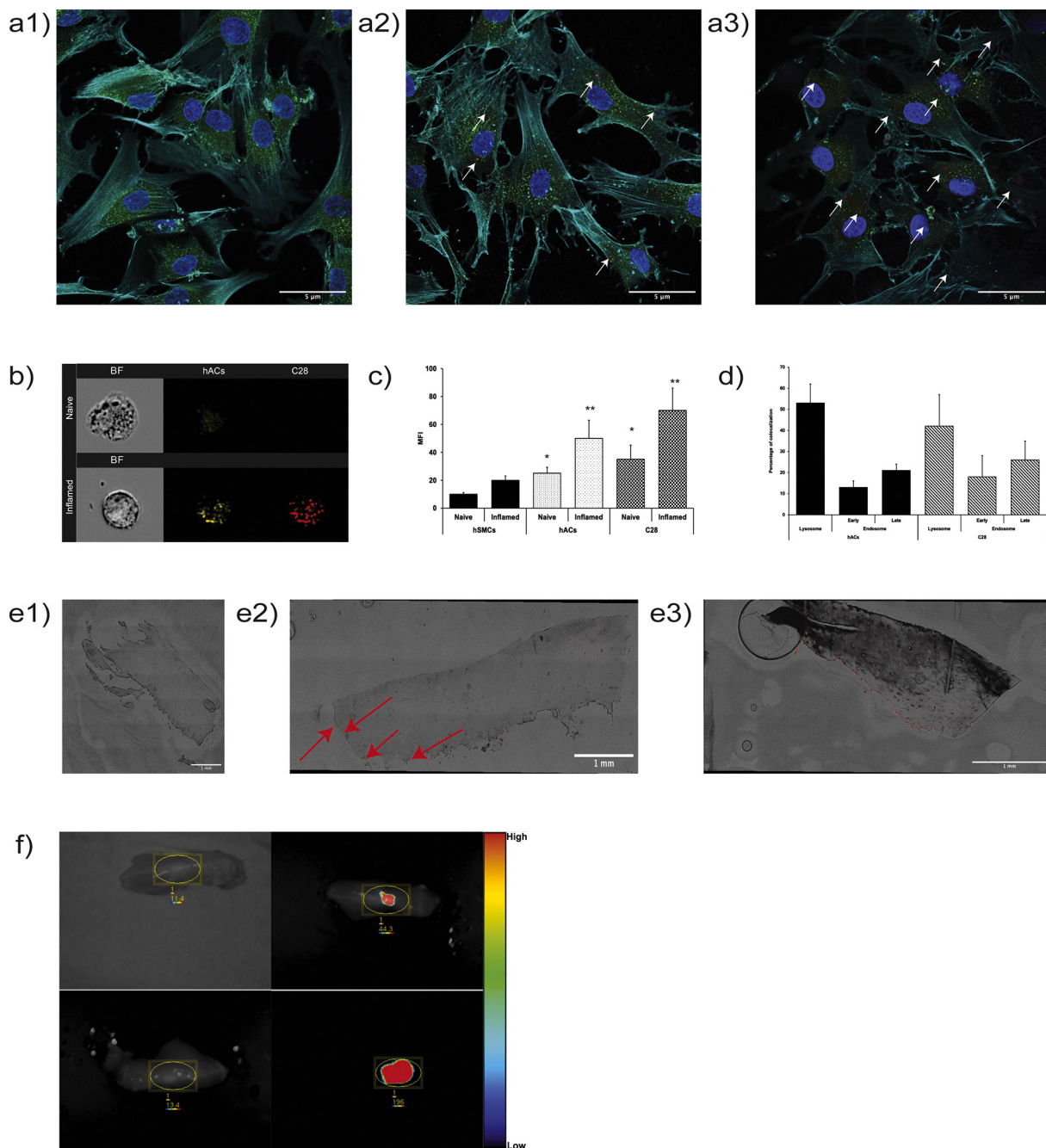


Fig. 3. NGs effect on cells viability.

Fig. a1 & a2: Alamar blue assay was used to assess NGs effect on hACs and C-28/I2 viability. Inflamed and naïve cells were incubated with 5 μ g/mL of NGs and the assay was performed every 24 h for 4 consecutive days. Inflamed cells were incubated with 10 ng/mL of TNF α prior incubation with NGs. The NGs cytotoxicity and their effect on cells' viability and cells' apoptosis was measured. (For interpretation of the references to colour in this figure legend, the reader is referred to the web version of this article.)

3.7. μ CT and histological analysis

Fourteen days post injection, the mice were sacrificed, and the limbs were collected and analyzed using a μ CT scanner. The results suggest that destabilization of medial menisci induced knee OA, and significant changes in the joint structures since osteophyte formation and cartilage degradation were observed (Fig. 5A). On the other hand, no osteophyte formations and cartilage degeneration were observed in healthy knees (Fig. 5A). The μ CT-scans of the knees injected with NGs showed less osteophyte formations and cartilage degeneration suggesting that NGs reduced OA development. To confirm the results of the CT-scan analysis,

the knees were also embedded in paraffin, cut and stained for Safranin-O/Fast Green and Hematoxylin/Eosin. The results confirmed the observations collected using the μ CT-scan: 1) the healthy knee did not show any osteophyte formation or cartilage degradation (Fig. 5B, top left); 2) the OA knee without treatment showed serious cartilage damages and osteophyte formation (Fig. 5B, top right); 3) the OA knee injected with NGs showed minor cartilage degradation and osteophyte formation (Fig. 5B, bottom right); and 4) the healthy knee injected with NGs did not show any changes compared to the healthy control (Fig. 5B, bottom left).

In addition to μ CT-scans and histological analysis the samples were

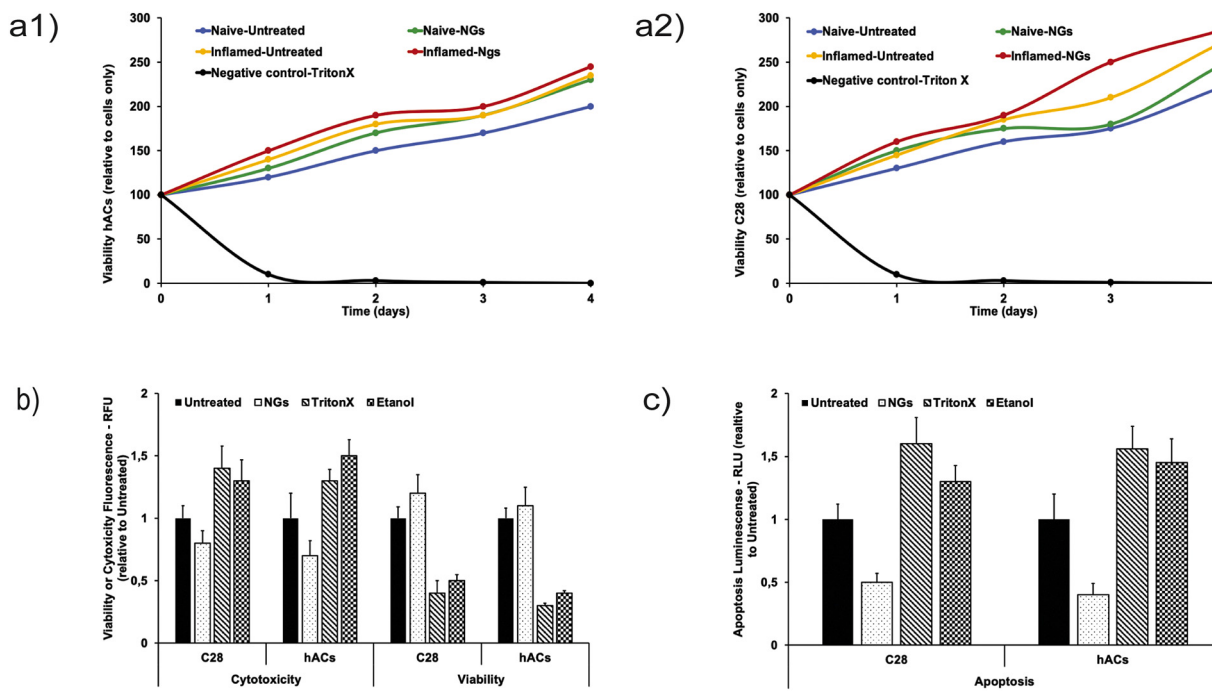


Fig. 4. NGs' immunomodulatory effect.

a) NO quantification. Naïve and inflamed hACs and C-28/I2 cells were incubated with NGs supplemented media (5 µg/mL) and the nitrite level were measured after 24 h of incubation using colorimetric Griess assay. NGs reduced NO levels of treated inflamed cells to naïve levels. The NGs did not affect the NO produced by naïve cells meaning that they did not stimulate any NO related to inflammatory process. b1) and b2) ELISA analysis of the inflammatory cytokines and PGE2. Naïve and inflamed hACs and C-28/I2 cells were incubated with NGs supplemented media (5 µg/mL) for 24 h. Inflamed cells were incubated with 10 ng/mL of TNFα prior incubation with NGs. After incubation the media were collected and ELISA assays against IL6 and IL8 cytokines and PGE2 were performed. c1) and c2) The effect of NGs (5 µg/mL) on mRNA expression of inflammation related genes (PGE2s, COX2, ADAMTS5, and MMP13) as measured in naïve and inflamed hACs and C-28/I2 cells. Inflamed cells were incubated with 10 ng/mL of TNFα prior incubation with NGs. The cells were incubated together with NGs for 24 h then harvested and the RNA was extracted, and RT-PCR analysis was performed for the mRNA expression of PGE2s ($P < 0.001$), COX2 ($P < 0.05$), ADAMTS5 ($P < 0.01$), and MMP13 ($P < 0.001$).

double blinded scored according to OARSI score in a double blinded setup. The sum of the averages of the medial compartment (femoral and tibia) and the lateral compartment (femoral and tibia) shows a three-folds reduction of the OA score in NG-injected knees while the maximum score reduced by 30% (Fig. 5 D4). The individual scores show that the medial part of Group 1 is less preserved than lateral part with a score of 2.4 and 1.8, respectively. This may be due to the site of injection of the NGs which was mainly localized in the lateral part, thus, dropping the score at the negative control levels.

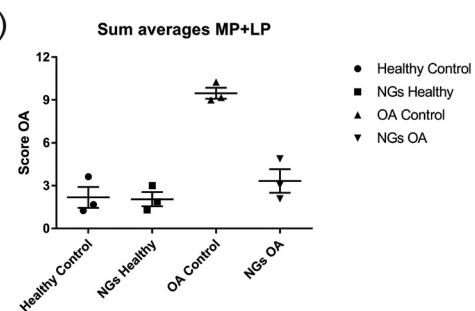
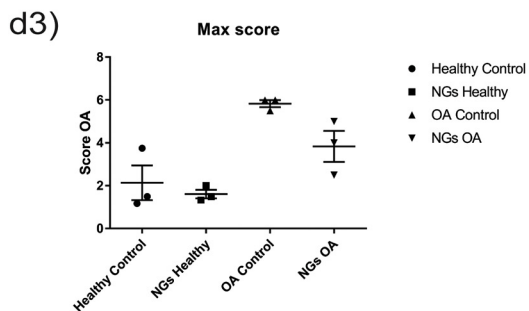
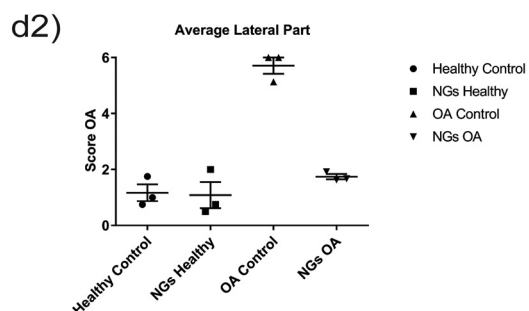
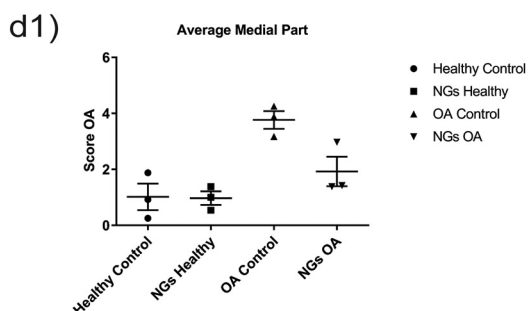
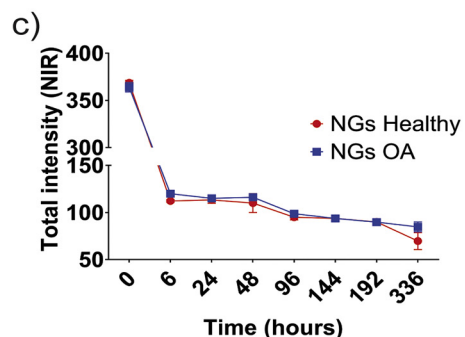
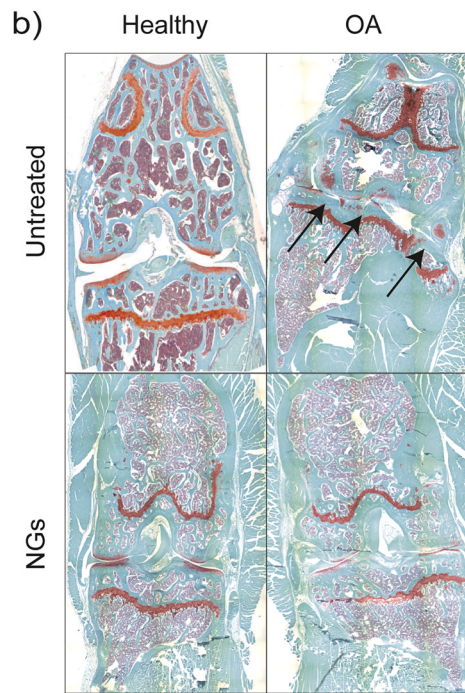
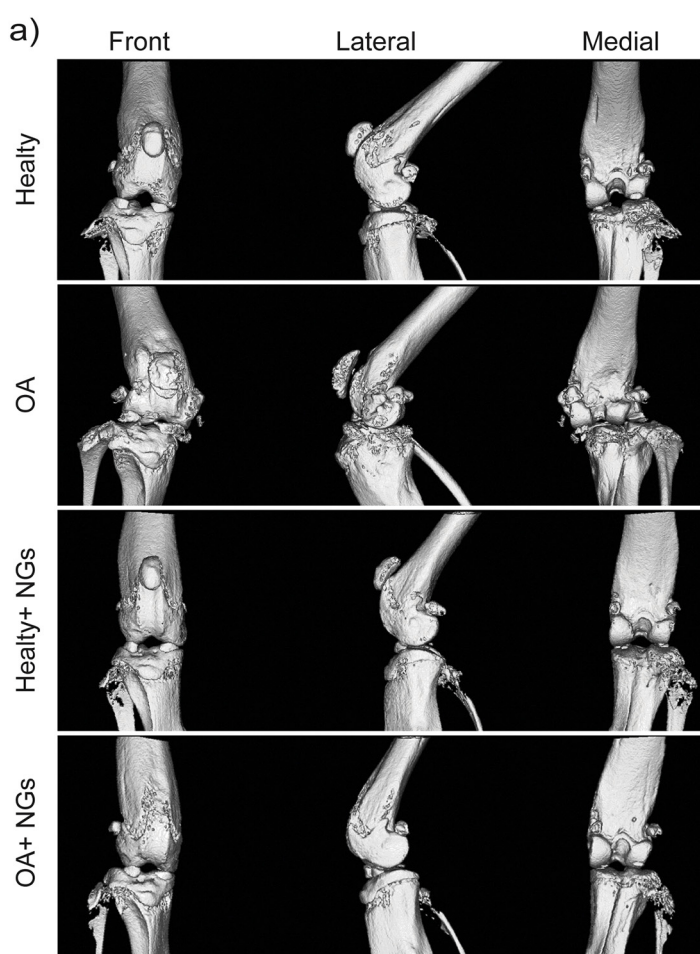
4. Discussion

To date, no current treatments address the underlying molecular causes of the OA. The most significative challenge for the treatment of OA remains the use of cell therapy or drug delivery approaches. In cell therapy, MSCs represent one of the main potential treatments for OA and they are considered a valid alternative to the current strategies as they could differentiate into cartilage and reconstitute the loss of the matrix. Nonetheless the complication rate and problem of MSCs based therapy received much attention over the years. Between 2005 and 2009, patients treated with MSCs to treat diseases of peripheral joints were diagnosed for neo plastic complications at any of the stem cells reimplantation site. In 2006, Agung et al. showed that the injection of 10^7 MSCs in OA sites did not improve the disease but rather generated free bodies of scar tissue. It is also uncertain whether the MSCs survive the implantation procedure or integrate with the newly formed tissue [19,20]. In terms of drug delivery approaches, the biggest problems are to overcome the lack of vasculature, the rapid clearance of locally delivered therapies (due to synovial fluid exchange), and the delivery of hydrophobic drugs. Many approaches have been tested, such as the use

of micelles, microparticles, micro-gels, liposomes and polymeric particles [21,22]. However, it has been shown that the use of these particles is not free of risks. Microparticles can induce inflammatory response and stimulate toxicity due to leftover of the solvents used for their synthesis [23–25]. In addition, micro- and nanoparticles may have a poor specificity in targeting. Therefore, some efforts have been done to increase this specific capability. For example, it has been shown that nanoparticles can be modified with positively charged avidin to increase the targeting towards the ECM which is negatively charged [26,27]. Another example is the modification of the nanoparticles using collagen II $\alpha 1$ -binding peptide (WYRGRL) which showed to increase the retention by 72 fold in murine joints [28].

In this study, we propose a novel approach that encompasses MSCs therapeutic advantages in a newly delivery technology that may serve as a platform for the treatment of OA. This approach is based on nanovesicles, termed NGs, that are produced from the cytoplasmic membrane of MSCs and preserve the cells' targeting capabilities towards inflammation sites. Thus, NGs may offer a possible future treatment platform for OA particularly by modulating the inflammatory process in the damaged tissue, while serving as a delivery platform for the delivery of therapeutics.

Our data demonstrate that the NGs possess the capability to target the cartilage under different conditions, and to preferentially target inflamed tissues. These NGs can be easily produced, depicting a spherical shape with 200 nm diameter and -12 mV Z-potential. One of the main problems of synthetic liposomes or polymeric nanoparticles is their immunogenicity [29–31], but due to the fact the NGs are derived from MSCs and their lack of internal machinery they can be considered safer than living cells and are not subjected to host induced changes [9,11–13]. The confirmation of NGs' advantages is the fact that they did



(caption on next page)

Fig. 5. NGs effect on OA mice.

a) CT-scan of knee joints. Mice legs were harvested and scanned using CT-scan machine. The 3D image of the leg was reconstructed via software. From the top of the image: A healthy NGs-untreated control, the untreated leg pictured from the front, the side, and the back. The cartilages between the femur and tibial bone are clearly untouched. OA NGs-untreated control: leg from a mouse that underwent a surgical DMM. Cartilages are destroyed and between the femur and the tibia is possible to see a new bone formation. Healthy NGs-treated control: there are no major differences compared to the negative control. OA NGs-treated control: leg from a mouse that underwent a surgical DMM. The OA developed slower compared to the OA NGs-untreated control. b) Mice legs where harvested, decalcified and embed in paraffin. Then, sliced and stained with Safranin-O fast green. Top left - healthy control, top right - OA control, bottom left - Healthy mice with NGs, bottom right: OA mice with NGs. c) 14 days post DMM surgery mice were injected with DiR labeled NGs (Ex: 750 nm, Em: 780 nm). The mice were scanned using a PEARL to identify possible NGs leakage to body. d) Quantitative evaluation of the NGs effect, using OARSI score, was performed on Saf-O/Fast-green stained samples. The score assesses 0 as perfect condition cartilage and 6 as destroyed cartilage (>75%). Each joint was divided to 4 parts: femur and tibial medial parts and femur and tibial later part and the averages of each part was calculated. As additional scores, the MAX score (the highest scores scored in a certain group independently by the compartments) and the SUM of MP and LP were calculated. Top left: average of the OA scores of the medial part (femur and tibia); Top right: average of the scores of the lateral part (femur and tibia), Bottom right: max OA score per knee, Bottom left: sum of OA score per knee of the medial and lateral compartments (femoral and tibial).

not affected the viability of chondrocytes, neither induced any apoptotic or necrotic process. NGs targeted chondrocyte cells and accumulated in their cytoplasm showing a preferential targeting towards inflamed cells. NGs showed their targeting abilities *in vitro* as well as *ex vivo*, where the preference to bind to inflamed cartilage was confirmed in rat knees, and human cartilage explants. Lastly, NGs showed, *in vivo*, to have superior targeting abilities and retained in the mice joint for over 14 days. This is superior other particles, such as iron particles which were shown to be cleared faster from the joint [32–34]. As MSCs are known to modulate inflammatory process [35–39], we aimed to test our hypothesis that the NGs, although lacking the cellular machinery, retain MSC membrane components and can exert anti-inflammatory capabilities which rely on cell-cell interaction [40,41].

First evidence to such effect is the NGs ability to reduce NO levels in inflamed cells. A more detailed analysis of our data clearly showed that the NGs can reduce inflammation at different levels affecting both protein and mRNA expression. PGE2 was one of the most affected markers by the NGs treatment. The expression level of PGE2 dropped significantly (three-fold, $P<0.01$) suggesting that the inflammatory pathway that involve COX2 and PGE2 is downregulated. Similar to the levels of PGE2, the levels of IL6 and IL8 cytokines where also reduced (two-folds, $p<0.05$) in inflamed cells after NGs treatment, confirming that NGs may interfere with the release of pro-inflammatory molecules in the medium downregulating the entire process.

A further confirmation of the effect of the NGs arises from the downregulation of PGE2 and COX2 transcripts in inflamed cells treated with NGs (Fig. 4). As with PGE2 and COX2, the levels of metalloproteases MMP13 and ADAMTS5 dropped significantly in inflamed cells after incubation with NGs (two-fold decrease, $P<0.001$), further supporting our previous results. Furthermore, the amount of mRNA levels of ECM-related genes such as ACAN increased as a possible confirmation of the healing process of chondrocytes. Reducing the inflammation at both RNA and protein levels, NGs showed that they effectively target and may interfere with the inflammatory pathway of different genes granting the ECM more time to repair itself. The increase of IL 6 in naïve cells may suggest that our NGs, retaining properties of MSCs membranes, bind to IL6 receptor as the MSCs themselves, and promote the activation of the pathway. At the same time, as it is for the COX2/PGE2 pathway, they seem to interfere with IL6 when the cells are inflamed by blocking the cascade and promoting a down-regulation.

Finally, our data showed that NGs also have a clear effect also *in vivo* by contributing to the preservation of the ECM. Their improved retention time in the joint, compared to liposome or synthetic nanoparticles, and their MSCs-derived capabilities seem to guarantee great targeting efficiency while preserving the ECM from destruction in NGs-injected OA-knees. The μCT-scan, histological analysis and scores, showed that the overall health of NGs-injected knees is comparable to healthy controls: the cartilage is thinner but still present, there is minimum formation of extra bone tissue and the overall score of the knees is comparable to the score of healthy knees. Altogether, our study introduce for the first time, a new and possible therapy for OA, which is based on our NGs technology, opening new research venues that exploite the

potential of NGs not only as a therapeutic but as a delivery system for additional therapeutics which can act in synergism with the ability of the NGs themselves to modulate the inflammatory process that is manifested in OA.

5. Conclusions

In this study we introduced, for the first time, a new approach to treat OA using a unique nanotechnology platform derived from mesenchymal stem cells, termed Nano-Ghosts. We have demonstrated that the NGs retained MSCs' membrane properties, as well as their homing properties to inflamed cells. Most importantly, we demonstrated the immunomodulatory characteristic of the NGs and their ability to play a major role in modulating the development of OA. The expression of cytokines associated with inflammation like IL6 and IL8, the expression of PGE2 that were dropped almost to naïve levels, as well as the drop of mRNA levels of inflammation related genes, and the *in vivo* data strongly attest to this conclusion, and to the future potential of the NGs as a therapeutic for OA. This data together with our previous published work, also provide first proof-of-concept not only for the use of NGs as a standalone biological but as a safe carrier platform for the selective delivery of therapeutics, such as anti-inflammatory drugs or regenerative factors.

Funding and credits

This project has received funding from the European Union's Horizon 2020 research and innovation program under Marie Skłodowska-Curie grant agreement No 642414.

This project has received funding from Technion Israel Institute of Technology.

The funding by the Dutch Arthritis Association (LLP12) is gratefully acknowledged.

This project used images (original one and modified) from Servier Medical Art by Servier.

Conflict of interests

The author M.M. is the inventor of the patent owned by the Technion Research and Development Foundation Ltd. (a subsidiary of the Technion IIT) entitled "Liposomal compositions and uses of same" that includes concepts presents here and which as granted in the US (US 9.642.817 B2) and the EU (EP 2470164 B1), and which is pending registration in China (CN 102596179) and India (484/ MUMNP/2012).

Credit authors statement

All the authors contributed equally to this research.

Acknowledgements

The completion of this project could not have been possible without the participation and assistance of so many people. Their contributions

are sincerely appreciated and gratefully acknowledged. However, a deep appreciation and special thanks to the following:

Dr. Gerjo J.V.M. van-Osch, Dr. Tomer Bronshtein, Dr. Nitsan Dahan, Dr. Galoz Kaneti, Sharbel Zahran, Tzila Davidov, Dr. Noa Cohen-Levy, Tom Givaty-Katz, Alex Ereskowsky, Ivo Que.

To all relatives, friends and other who in one way or another shared their support, either morally or physically, thank you.

Appendix A. Supplementary data

Supplementary data to this article can be found online at <https://doi.org/10.1016/j.jconrel.2021.05.015>.

References

- [1] S.M. Sheila, K.C. Duncan, A.M. Lynch, Osteoarthritis: a review of treatment options, *Geriatrics*. 64 (2009) 20–29.
- [2] I. Haq, E. Murphy, J. Dacre, Osteoarthritis, *Postgrad. Med. J.* 79 (2003) 377–383.
- [3] M.B. Goldring, M. Otero, Inflammation in osteoarthritis, *Curr. Opin. Rheumatol.* 23 (2011) 471.
- [4] S. Park, E.G. Lakatta, Role of inflammation in the pathogenesis of osteoarthritis, *Yonsei Med. J.* 53 (2013) 258–261.
- [5] F. Barry, M. Murphy, Mesenchymal stem cells in joint disease and repair, *Nat. Rev. Rheumatol.* 9 (2013) 584–594.
- [6] J.C. Snibbe, R.A. Gambardella, Treatment options for osteoarthritis, *Orthopedics*. 28 (2005) s215–20.
- [7] K.A. Dewing, S.M. Setter, B.A. Slusher, Osteoarthritis and rheumatoid arthritis 2012: pathophysiology, diagnosis, and treatment, *Clin. Adv. 15* (2012) 44.
- [8] J.L. Escobar Ivirico, M. Bhattacharjee, E. Kuyinu, L.S. Nair, C.T. Laurencin, Regenerative engineering for knee osteoarthritis treatment: biomaterials and cell-based technologies, *Engineering*. 3 (1) (2017) 16–27.
- [9] N. Letko Khait, N. Malkah, G. Kaneti, L. Fried, N. Cohen Anavy, T. Bronshtein, M. Machluf, Radiolabeling of cell membrane-based nano-vesicles with 14C-linoleic acid for robust and sensitive quantification of their biodistribution, *J. Control. Release* 293 (2019) 215–223.
- [10] M. Timaner, N. Letko-Khait, R. Kotofruk, M. Benguigui, O. Beyar-Katz, C. Rachman-Tzemah, Z. Raviv, T. Bronshtein, M. Machluf, Y. Shaked, Therapy-educated mesenchymal stem cells enrich for tumor-initiating cells, *Cancer Res.* 78 (2018) 1253–1265.
- [11] L. Kaneti, T. Bronshtein, N. Malkah Dayan, I. Kovregina, N. Letko Khait, Y. Lupu-Haber, M. Fliman, B.W. Schoen, G. Kaneti, M. MacHluf, Nanoghosts as a novel natural nonviral gene delivery platform safely targeting multiple cancers, *Nano Lett.* 16 (2016) 1574–1582.
- [12] N.E. Toledo Furman, Y. Lupu-Haber, T. Bronshtein, L. Kaneti, N. Letko, E. Weinstein, L. Baruch, M. Machluf, Reconstructed stem cell nanoghosts: a natural tumor targeting platform, *Nano Lett.* 13 (2013) 3248–3255.
- [13] J. Oieni, A. Lolli, D. D'Atri, N. Kops, A. Yayon, J.V.M.G. van Osch, M. Machluf, Nano-ghosts: Novel biomimetic nano-vesicles for the delivery of antisense oligonucleotides, *Journal of controlled release* 333 (2021) 28–40.
- [14] C. Ha, S. Tian, K. Sun, D. Wang, J. Lv, Y. Wang, Hydrogen sulfide attenuates IL-1 β -induced inflammatory signaling and dysfunction of osteoarthritic chondrocytes, *Int. J. Mol. Med.* 35 (2015) 1657–1666.
- [15] J. Schwager, U. Hoeller, S. Wolfram, N. Richard, Rose hip and its constituent galactolipids confer cartilage protection by modulating cytokine, and chemokine expression, *BMC Complement. Altern. Med.* 11 (2011) 105.
- [16] M.G. Neuman, N.H. Shear, R.G. Cameron, G. Katz, C. Tiribelli, Ethanol-induced apoptosis in vitro, *Clin. Biochem.* 32 (1999) 547–555.
- [17] H. Iturriaga, S. Vaisman, M.E. Pino, T. Pereda, Lysosomal injury and hepatic necrosis: effects of triton WR-1339 on liver cells in the rat, *Exp. Mol. Pathol.* 14 (1971) 350–361.
- [18] M.M. Börner, E. Schneider, F. Pirnia, O. Sartor, J.B. Trepel, C.E. Myers, The detergent triton X-100 induces a death pattern in human carcinoma cell lines that resembles cytotoxic lymphocyte-induced apoptosis, *FEBS Lett.* 353 (1994) 129–132.
- [19] W. Yan, Y. Qi, G. Feng, Mesenchymal stem cell-based treatment for cartilage defects in osteoarthritis Use of iNSC and neurosteroids for the treatment of spinal cord injury View project Mesenchymal stem cell-based treatment for cartilage defects in osteoarthritis, *Artic. Mol. Biol. Reports.* 39 (2012) 5683–5689.
- [20] M. Agung, M. Ochi, S. Yanada, N. Adachi, Y. Izuta, T. Yamasaki, K. Toda, Mobilization of bone marrow-derived mesenchymal stem cells into the injured tissues after intraarticular injection and their contribution to tissue regeneration, *Knee Surg. Sport. Traumatol. Arthrosc.* 14 (2006) 1307–1314.
- [21] L.S. Lohmander, E.M. Roos, Clinical update: treating osteoarthritis, *Lancet.* 370 (2007) 2082–2084.
- [22] W. Zhang, R.W. Moskowitz, G. Nuki, S. Abramson, R.D. Altman, N. Arden, S. Bierma-Zeinstra, K.D. Brandt, P. Croft, M. Doherty, M. Dougados, M. Hochberg, D.J. Hunter, K. Kwoh, L.S. Lohmander, P. Tugwell, OARSI recommendations for the management of hip and knee osteoarthritis, part II: OARSI evidence-based, expert consensus guidelines, *Osteoarthr. Cartil.* 16 (2008) 137–162.
- [23] F. Shu, Y. Shi, Systematic overview of solid particles and their host responses, *Front. Immunol.* 9 (2018).
- [24] S.R. Mulay, M. Herrmann, R. Bilyy, A. Gabibov, H.-J. Anders, Editorial: nano- and microparticle-induced cell death, inflammation and immune responses, *Front. Immunol.* 10 (2019) 844.
- [25] B.H. Fellah, D. Chappard, P. Weiss, N. Josselin, P. Layrolle, B.H. Fellah, P. Weiss, P. Layrolle, N.D. Josselin Chappard, Inflammatory reaction in rats muscle after implantation of biphasic calcium phosphate micro particles H2020 MCSA-IF: biomaterials with incorporated MSC-secreted PARAcrine molecules for bone reGENERation view project injectable calcium phosphate for TE View project inflammatory reaction in rats muscle after implantation of biphasic calcium phosphate micro particles, *Artic. J. Mater. Sci. Mater. Med.* 18 (2007) 287–294.
- [26] A.G. Bajpayee, M.A. Quadir, P.T. Hammond, A.J. Grodzinsky, Charge based intra-cartilage delivery of single dose dexamethasone using Avidin nano-carriers suppresses cytokine-induced catabolism long term, *Osteoarthr. Cartil.* 24 (2016) 71–81.
- [27] A.G. Bajpayee, M. Scheu, A.J. Grodzinsky, R.M. Porter, Electrostatic interactions enable rapid penetration, enhanced uptake and retention of intra-articular injected avidin in rat knee joints, *J. Orthop. Res.* 32 (2014) 1044–1051.
- [28] D.A. Rothenfluh, H. Bermudez, C.P. O'Neil, J.A. Hubbell, Biofunctional polymer nanoparticles for intra-articular targeting and retention in cartilage, *Nat. Mater.* 7 (2008) 248–254.
- [29] S. Dwivedi, D. Ahirwar, P. Tiwari, 9 Adverse Immune Effects of Liposomes: Immunogenicity and Immune Suppression, n.d.
- [30] N. Monteiro, A. Martins, R.L. Reis, N.M. Neves, Liposomes in tissue engineering and regenerative medicine, *J. R. Soc. Interface* 11 (2014) 20140459.
- [31] S.C. Semple, T.O. Harasym, K.A. Clow, S.M. Ansell, S.K. Klimuk, M.J. Hope, Immunogenicity and rapid blood clearance of liposomes containing polyethylene glycol-lipid conjugates and nucleic acid, *J. Pharmacol. Exp. Ther.* 312 (2005) 1020–1026.
- [32] R. Labens, C. Daniel, S. Hall, X.R. Xia, T. Schwarz, Effect of intra-articular administration of superparamagnetic iron oxide nanoparticles (SPIONs) for MRI assessment of the cartilage barrier in a large animal model, *PLoS One* 12 (2017).
- [33] R.E. Whitmire, D. Scott Wilson, A. Singh, M.E. Levenston, N. Murthy, A.J. García, Self-assembling nanoparticles for intra-articular delivery of anti-inflammatory proteins, *Biomaterials*. 33 (2012) 7665–7675.
- [34] T.W.G.M. Spitters, D. Stamatialis, A. Petit, M.G.W. De Leeuw, M. Karperien, In vitro evaluation of small molecule delivery into articular cartilage: effect of synovial clearance and compressive load, *Assay Drug Dev. Technol.* 17 (2019) 191–200.
- [35] S. Aggarwal, M.F. Pittenger, Human mesenchymal stem cells modulate allogeneic immune cell responses, *Blood*. 105 (2005) 1815–1822.
- [36] X. Zhang, F. Huang, W. Li, J.L. Dang, J. Yuan, J. Wang, D.L. Zeng, C.X. Sun, Y. Liu, Q. Ao, H. Tan, W. Su, X. Qian, N. Olsen, S.G. Zheng, Human gingiva-derived mesenchymal stem cells modulate monocytes/macrophages and alleviate atherosclerosis, *Front. Immunol.* 9 (2018).
- [37] A. Amouzegar, S.K. Mittal, A. Sahu, S.K. Sahu, S.K. Chauhan, Mesenchymal stem cells modulate differentiation of myeloid progenitor cells during inflammation, *Stem Cells* 35 (2017) 1532–1541.
- [38] M.Y. Noh, S.M. Lim, K.-W. Oh, K.-A. Cho, J. Park, K.-S. Kim, S.-J. Lee, M.-S. Kwon, S.H. Kim, Mesenchymal stem cells modulate the functional properties of microglia via TGF- β secretion, *Stem Cells Transl. Med.* 5 (2016) 1538–1549.
- [39] E. Gerdoni, B. Gallo, S. Casazza, S. Musio, I. Bonanni, E. Pedemonte, R. Mantegazza, F. Frassoni, G. Mancardi, R. Pedotti, A. Uccelli, Mesenchymal stem cells effectively modulate pathogenic immune response in experimental autoimmune encephalomyelitis, *Ann. Neurol.* 61 (2007) 219–227.
- [40] M. Wang, Q. Yuan, L. Xie, Mesenchymal stem cell-based immunomodulation: properties and clinical application, *Stem Cells Int.* 2018 (2018).
- [41] Y. Li, D. Zhang, L. Xu, L. Dong, J. Zheng, Y. Lin, J. Huang, Y. Zhang, Y. Tao, X. Zang, D. Li, M. Du, Cell-cell contact with proinflammatory macrophages enhances the immunotherapeutic effect of mesenchymal stem cells in two abortion models, *Cell. Mol. Immunol.* 16 (2019) 908–920.